Cerebral Cortex January 2008;18:1-12
doi:10.1093/cercor/bhm026
Advance Access publication March 29, 2007

D_1 but not D_5 Dopamine Receptors Are Critical for LTP, Spatial Learning, and LTP-Induced arc and zif268 Expression in the Hippocampus

Noelia Granado[1], Oskar Ortiz[1], Luz M. Suárez[2], Eduardo D. Martín[3], Valentín Ceña[3], José M. Solís[2] and Rosario Moratalla[1]

[1]Instituto Cajal, Consejo Superior de Investigaciones Científicas, 28002 Madrid, Spain, [2]Hospital Ramón y Cajal, 28034 Madrid, Spain and [3]Departamento de Ciencias Médicas, Universidad de Castilla-La Mancha, 02006 Albacete, Spain

Noelia Granado, Oskar Ortiz, and Luz M. Suárez contributed equally in this work

Recent evidence suggests that glutamatergic and dopaminergic afferents must be activated to induce persistent long-term potentiation (LTP) in the hippocampus. Whereas extensive evidence supports the role of glutamate receptors in long-lasting synaptic plasticity and spatial learning and memory, there is less evidence regarding the role of dopamine receptors in these processes. Here, we used dopamine D_1 receptor knockout ($D_1R^{-/-}$) mice to explore the role of D_1R in hippocampal LTP and its associated gene expression. We show that the magnitude of early and late phases of LTP (E-LTP and L-LTP) was markedly reduced in hippocampal slices from $D_1R^{-/-}$ mice compared with wild-type mice. SCH23390, a D_1/D_5R antagonist, did not further reduce L-LTP in $D_1R^{-/-}$ mice, suggesting that D_5Rs are not involved. $D_1R^{-/-}$ mice also showed a significant reduction of D_1R-induced potentiation of N-Methyl-D-aspartic acid-mediated currents, via protein kinase activated by cyclic adenosine 3′,5′-monophosphate activation. Finally, LTP-induced expression of the immediate early genes *zif268* and *arc* in the hippocampal CA1 area was abolished in $D_1R^{-/-}$ mice, and these mice showed impaired learning. These results indicate that D_1R but not D_5R are critical for hippocampal LTP and for the induction of Zif268 and Arc, proteins required for the transition from E-LTP to L-LTP and for memory consolidation in mammals.

Keywords: behavior, cognition, dopamine, knockout, LTP, memory, water maze

Introduction

Glutamate receptors, in particular the NMDA receptor (NMDAR), are known to be central to long-term potentiation (LTP), learning, and memory (Malenka and Bear 2004). However, increasing evidence suggests that dopamine is also involved in the expression of activity-dependent synaptic plasticity as well as in behavioral learning and learning-associated immediate-early gene expression (O'Carroll and Morris 2004; Lisman and Grace 2005). Intact dopaminergic input is necessary for long-term changes in synaptic efficacy in different brain areas including the cortex (Gurden et al. 1999; Huang et al. 2004), the striatum (Calabresi et al. 1992; Picconi et al. 2003), and the hippocampus (Huang and Kandel 1995; Li et al. 2003). Similarly, normal dopaminergic activity appears essential for various forms of learning and memory because dopaminergic dysfunction in the prefrontal cortex or the hippocampal formation significantly alters spatial learning, goal-related behavior, and short- and long-term memory in rodents and nonhuman primates (Whishaw and Dunnet 1985; Williams and Goldman-Rakic 1995).

It is still unclear whether LTP is the mechanistic underpinning of memory, although much evidence is consistent with the notion that it underlies the formation and initial storage of associative memory (Pastalkova et al. 2006; Whitlock et al. 2006). The hippocampus, which plays a key role in associative memory networks and spatial memory, is the site of well-documented long-lasting changes in synaptic plasticity and receives strong dopaminergic input from midbrain dopaminergic neurons (Huang et al. 1992). It has been shown that exposure to novelty, a phenomenon known to release dopamine (Ljungberg et al. 1992), facilitates dopamine-dependent LTP induction (Li et al. 2003) via D_1-class receptors (D_1/D_5R). Studies in D_1 receptor knockout ($D_1R^{-/-}$) mice suggest that this receptor is essential for spatial memory tasks (Smith et al. 1998; El-Ghundi et al. 1999) and LTP maintenance (Matthies et al. 1997). However, the specific roles played by D_1R and D_5R in LTP are unknown due to the lack of ligands able to discriminate between these 2 receptors. Nevertheless, by using antagonists against D_1/D_5Rs, it has been concluded that the activation of any of these receptors is crucial for the enduring synaptic changes observed during the late phase of LTP (L-LTP) (Frey et al. 1991; Huang and Kandel 1995; Swanson-Park et al. 1999; Lemon and Manahan-Vaughan 2006). This L-LTP is dependent on new protein synthesis and lasts more than 3 h (Sajikumar et al. 2005). However, the role of D_1/D_5Rs in early LTP (E-LTP), which is protein synthesis independent, is less clear. Whereas some authors found no effect of D_1/D_5R antagonist on E-LTP (Huang and Kandel 1995; Huang et al. 2004), others found that D_1/D_5R activation enhances E-LTP (Otmakhova and Lisman 1996). Among the genes activated for the transition from E-LTP to L-LTP, the IEGs *zif268* and *arc* (activity-regulated cytoskeletal protein) are critical and have been implicated in the expression of long-term memories (Guzowski et al. 2000; Jones et al. 2001) and glutamate- and dopamine-mediated synaptic plasticity (Moratalla et al. 1992; 1996; Konradi et al 1996; Tan et al. 2000; Pavón et al. 2006; Rodrigues et al. 2007).

In the present study, we used genetically engineered mice lacking the D_1R to establish the role of D_1 and D_5 dopamine receptors on synaptic plasticity, E- and L-LTP, and in the activity-dependent gene expression of *zif268* and *arc* associated with both, synaptic plasticity and learning and memory processes.

Materials and Methods

Animals

Mice lacking the dopamine D_1R were generated by homologous recombination as described previously (Xu et al. 1994; Moratalla et al. 1996). Male and female wild-type (WT) and homozygote $D_1R^{-/-}$ mice used in this study were derived from the mating of heterozygous mice. Genotype was determined by Southern blot analysis (Xu et al. 1994). All mice were 4–6 months old and were housed in groups of 6 per cage in a temperature-controlled room (22 °C) on a 12-h dark–light cycle with

free access to food and water. Animals were treated in accordance with European Community guidelines (86/609/ECC), and the procedures were approved by the Bioethical Committee at the Cajal Institute.

Pharmacological Agents and Reagents

DL-2-amino-5-phosphopentanoic acid (AP5), bicuculline methiodide (BMI), and 6-cyano-7-nitroquinoxaline-2,3-dione disodium (CNQX) were obtained from Sigma (Madrid, Spain); KT5720, SCH23390, and SKF81297 from Tocris (Avonmouth, UK). Drugs were prepared as stock solutions, stored frozen in the dark, and diluted to final concentration immediately before use. Stock solutions of AP5 (25 mM), CNQX (20 mM), and SCH23390 (1 mM) were prepared in distilled water. Stock solutions of KT5720 (1 mM) were prepared in dimethyl sulfoxide.

Extracellular Recordings

Transverse hippocampal slices (400 μm) were prepared from female and male mice (12–18 weeks old) using conventional methods. $D_1R^{-/-}$ mice and WT mice were used on alternate days. Mice were anesthetized with halothane and decapitated. Hippocampi were removed and dropped in ice-cold Krebs–Ringer bicarbonate (KRB) solution containing (in mM) the following: 119 NaCl, 26.2 $NaHCO_3$, 2.5 KCl, 1 KH_2PO_4, 1.3 $MgSO_4$, 2.5 $CaCl_2$, and 11 glucose. This solution was pregassed with 95% O_2 and 5% CO_2. The dorsal hippocampi were sliced with a manual tissue chopper and placed in a holding chamber for more than 3 h at room temperature. A single slice was transferred to a submersion recording chamber, where it was continuously perfused (1.8–2 mL/min) with KRB warmed to 31–32 °C.

Extracellular field excitatory postsynaptic potentials (fEPSPs) were recorded with a tungsten microelectrode (1 MΩ) positioned in the stratum radiatum of CA1 area and connected via a headstage (AI-401, Axon Instruments, Foster City, CA) to a CyberAmp 320 signal conditioner (Axon Instruments). Field EPSPs were evoked by stimulating Schaffer collateral–commisural (SCC) axons with biphasic electrical pulses (20–60 μA, 100 μs, and 0.066 Hz) delivered through bipolar tungsten microelectrodes (0.5 MΩ) placed in CA1 midstratum radiatum. Electrical pulses were supplied by a pulse generator AMPI Mod Master 8 (Jerusalem, Israel) connected to a biphasic stimulus isolator unit in constant current mode (Cibertec, Madrid, Spain). Stimulation intensity was adjusted to evoke fEPSP slopes that were 40% of the maximal responses. A stable baseline was recorded during at least 20 min. Data were normalized with respect to the mean values of fEPSP slope recorded during this period. E-LTP was induced by a high-frequency stimulation (HFS) train (100 Hz, 1 s, at test intensity) and L-LTP by 3 HFS trains at 10-min intervals. Evoked responses were digitized at 25 kHz using a Digidata 1200AE-BD or 1320A (Axon Instruments) board running Clampex-8.0.2 software (Axon Instruments). The synaptic strength was calculated using the initial rising slope phase (0.7-ms window) of the fEPSP to avoid possible contamination of the response by propagated population spikes. As baseline for field potentials, we considered the mean value of the signal (2–5 ms) preceding the stimulus artifact. We used pCLAMP-8.0.2 software for these calculations. Traces shown are averages of 8 consecutive responses. Data were normalized with respect to the mean values of fEPSP slope recorded during the last 20 min of the baseline period in standard medium.

Whole-Cell Recordings

Whole-cell recordings from CA1 hippocampal pyramidal neurons were made using the patch-clamp technique as previously described (Martin and Buño 2003). Slices were transferred to an immersion recording chamber placed in an Axioskop upright microscope (Carl Zeiss, Göttingen, Germany) equipped with infrared and differential interference contrast imaging devices and with a 40× water immersion lens and superfused (2 mL/min) with gassed KRB. Patch electrodes had a resistance of 4–6 MΩ when filled with the internal solution that contained (in mM) the following: K-gluconate 97.5, KCl 32.5, ethyleneglycol-bis(2-aminoethylether)-*N,N,N′,N′*-tetraacetic acid 5, 4-(2-hydroxyethyl)-1-piperazineethanesulfonic acid 10, $MgCl_2$ 1, ATP 4, and QX-314 5, pH 7.2–7.3, osmolarities between 280 and 290 mOsm/L. Whole-cell recordings in the voltage-clamp modes were obtained with an Axopatch 200A amplifier (Axon Instruments). Fast and slow capacitances were neutralized, series resistance was compensated (≈70%), and membrane potential (Vm) was held at –60 mV. Data were discarded if the series resistance changed by more than 20% during an experiment. Bipolar Elgiloy electrodes (SSM33A05, WPI, Hertfordshire, UK) were placed in the stratum radiatum near the border of CA1 pyramidal layer to stimulate SCC. Stimuli were single pulses delivered at 0.3 Hz via an S-900 stimulator and S-910 isolation unit (Dagan Corporation, Minneapolis, MN). Pharmacologically isolated NMDA excitatory postsynaptic currents (NMDA EPSCs) were obtained by recording in Mg^{2+}-free external solution to remove the block of the NMDAR channel by extracellular Mg^{2+} and by blocking γ-aminobutyric acid A ($GABA_A$) receptors with BMI (50 μM) and α-amino-3 hydroxy-5 methylisooxazole-4 propionic acid (AMPA) receptors with CNQX (20 μM). Data were filtered at 2 KHz and transferred to the hard disk of a Pentium-based computer using a DigiData 1322A interface and the pCLAMP 9.0 software (Axon Instruments).

Spatial Navigation: Morris Water Maze

Spatial learning and memory were assessed in $D_1R^{-/-}$ mice (n = 15) and WT (n = 15) littermates using the Morris water maze. The maze consisted of a circular tank (100 cm diameter) filled with 21 °C water located in a room with visible external cues. A hidden escape platform (6 × 6 × 33 cm), made of roughened Plexiglas, was submerged 1 cm under water in 1 of the 4 designated positions within the tank. During the acquisition trials (days 1–6), mice were trained to escape from water by swimming from variable starting points around the tank to the hidden platform and allowed to remain there for 15 s. Mice failing to find the platform within 60 s were guided to the platform and placed on it for 15 s. After each trial, mice were dried and returned to their home cages. All sessions were recorded by a video camera located above the tank. Mice received 4 trials per day, for 6 consecutive days, with an intertrial interval of 5–7 min, and their escape latency was recorded for each trial. In the probe trials (no platform), conducted on the first day (day 1) and 72 h after the last acquisition trial (day 9), mice were allowed to swim for 60 s. Time spent in the target quadrant, number of annulus crossings through the previous platform location, and swimming speed were recorded. Following the probe trial on day 9, all mice were given reversal trials in which the hidden platform was relocated diagonally to the previous position. A total of 12 trials over 3 consecutive days (day 9–11), 4 trials per day, were given, and escape latencies were recorded. In another experiment, naive groups of mice were subjected to cued training trials test and were trained to find a submerged platform marked with a local visible cue to test their nonspatial learning ability, motivation, and sensorimotor coordination. All mice were given a series of 8 trials over 2 consecutive days.

Locomotor Activity and Sensorimotor Tasks

Basal horizontal and vertical movements were recorded for $D_1R^{-/-}$ mice (n = 22) and WT (n = 22) littermates as indicated (Xu et al. 1994; Centonze et al. 2003) using a multicage activity meter (Columbus Instruments, Columbus, OH) with a set of 8 individual cages measuring 20 × 20 × 28 cm. Horizontal movement was detected by 2 arrays of 16 infrared beams, whereas a third array positioned 4 cm above the floor detected vertical movement. The software allowed a distinction to be made between repetitive interruptions of the same photobeam and interruptions of adjacent photobeams. This latter measure was used as an index of ambulatory activity. Mice were habituated to the cages in 15-min sessions for 3 days. During the test session, beam breaks were recorded for 60 min as a measure of basal locomotor activity.

Visual acuity was assessed by the ability of a mouse to extend its forepaws when lowered gently by the tail toward a black surface as indicated by Lamberty and Gower (1990) in both genotypes of mice (n = 15 per genotype). Motor coordination was measured in the rotarod test (Ugo Basile, Rome, Italy) at fixed speed on 2 consecutive days. On each day, mice had a 10-min training session. The mouse was placed in the immobile rod, and the speed was turned on to 10 rpm. If the mouse fell from the rotarod during the training session, it was placed back on. Two hours after the training session, the performance of the mice was tested in a 3-min session. The latency to fall of the rotating rod was measured for all animals in the 2 consecutive days.

Immunohistochemistry and Quantification Analysis for the Immediate-Early Genes zif268 *and* arc *Induced after Tetanus*

Appropriate transverse hippocampal slices used in the electrophysiology studies were fixed in 4% paraformaldehyde overnight and cut into

40-μm sections. Immunohistochemistry was done in free-floating sections with standard avidin–biotin immunocytochemical protocols (Rivera et al 2002, Grande et al. 2004; Pavón et al. 2006) with specific polyclonal rabbit antisera raised against Zif268 (diluted 1:400) or against Arc (diluted 1:400) from Santa Cruz Biotechnology, Santa Cruz, CA. To enhance the stainings, after incubation with the primary (2 nights) and secondary (2 h) antisera, sections were incubated for 1 h in a streptavidin–peroxidase complex (Sigma, diluted 1:2000 in phosphate-buffered saline-TX). Peroxidase reactions were developed in 0.05% 3,3′-diaminobenzidine (DAB, Sigma) and 0.002% H_2O_2 for Zif268 or DAB plus nickel ammonium sulfate (Arc). Sections were then mounted on gelatin-coated slides, air dried, dehydrated in graded series of ethanol, cleared in xylene, and coverslipped with Permount mounting medium. Quantification analysis for Zif268- and Arc-positive nuclei in hippocampal sections was performed with the aid of an image analysis system (Analytical Imaging Station, Imaging Research Inc., Linton, UK) using a 40× lens. Before counting, images were thresholded at a standardized gray-scale level, empirically determined by 2 different observers to allow detection of stained nuclei from low to high intensity, with suppression of the very lightly stained nuclei. Thus, the number of positive nuclei for Zif268 and Arc was determined and was expressed as number of positive nuclei per square millimeter. Counts were obtained from 3 (Arc) and 4 (Zif268) hippocampal slices, each from a different animal and with 4–7 sections each slice. We considered $n = 3$ (Arc) or $n = 4$ (Zif268) for statistical analysis. For the experiments pertaining to the pharmacological blockage of D_1Rs during tetanus, we used 3 different sets of experiments (3 slices each), in which slices from WT animals were stimulated and recorded in the presence of 0.5 μM SCH23390 or standard KRB. Basal conditions were obtained from nonstimulated hippocampal sections maintained in the recording chamber.

Statistical Analysis

Data are presented as mean ± standard error of mean. Statistics on behavioral values to assess genotype and trial differences in the water maze or differences between mean fEPSP slopes were performed using repeated measures 2-way analysis of variance where mice genotype (WT and $D_1R^{-/-}$mice) and time (day of trials for water maze, or minutes after tetanus for electrophysiological studies) were entered as independent variables. Relevant differences were analyzed pair wise by post hoc comparisons with Tukey's test or Bonferroni's test. Normalized EPSP amplitudes, quadrant preferences, rotarod fall latencies, and motor activity were analyzed using the Student's *t*-test. For all statistical studies, a SigmaStat 2.03 program was used, and the threshold for statistical significance was set up at $P < 0.05$). SigmaPlot 9.0 software was used for graphics making.

Results

Schaffer Collateral -CA1 Pyramidal Neuron Synapses in $D_1R^{-/-}$ Mice Exhibit Normal Basal Synaptic Transmission and Paired-Pulse Facilitation

We first established that basal SCC-evoked fEPSPs are similar in both types of mice. Under our experimental conditions, fEPSPs predominantly reflect the activation of AMPA glutamate receptors. We performed stimulus/response curves using a range of stimulus intensities (5–100 μA) in slices from WT ($n = 14$) and $D_1R^{-/-}$ ($n = 11$) mice. There was no significant difference between these groups at any stimulus strength ($F_{1,124} = 0.11$, $P = 0.7423$, Fig. 1*A*). We also examined paired-pulse facilitation, consisting of pairs of homosynaptic stimuli separated by a short interval (20–250 ms). This kind of facilitation is caused by presynaptic mechanisms and has been used to detect changes in the synaptic release of glutamate (Issacson et al. 1993). The paired-pulse facilitation ratio in $D_1R^{-/-}$ mice was statistically indistinguishable from that evoked in WT mice (Fig. 1*B*, $F_{1,105} = 1.78$, $P = 0.1845$). These results indicate that the basal characteristics of excitatory synaptic transmission at SCC–CA1 pyramidal neuron synapses are not altered in $D_1R^{-/-}$ mice.

E-LTP Magnitude Is Reduced in $D_1R^{-/-}$ Mice

We next examined whether disruption of D_1R expression affects the E-LTP induction. In WT mice ($n = 6$), the application of a single train of tetanization (100 Hz, 1 s) induced a slowly decaying synaptic potentiation that returned to baseline values about 80 min after the tetanus (Fig. 2*A*,*A*′). This potentiation matches the time course for E-LTP described by other authors (Abel et al. 1997). When the same tetanus was applied to slices from $D_1R^{-/-}$ mice ($n = 5$), the resulting E-LTP was significantly smaller than in WT animals: at 60 min after tetanus, potentiation in $D_1R^{-/-}$ mice was 103 ± 4 versus 118 ± 5% in WT ($P < 0.05$, Fig. 2*A*′). In addition, the potentiation in $D_1R^{-/-}$ mice decayed faster than in WT mice, returning to baseline at 50–60 min after tetanus versus 90 min in WT animals. The difference in the magnitude of potentiation obtained in WT and $D_1R^{-/-}$ mice was evident as early as 5–10 min after tetanus and remained statistically significant for the entire duration of the early phase ($P < 0.05$, Fig. 2*A*′), indicating that the lack of D_1Rs affects early mechanisms of LTP induction.

L-LTP Is Reduced in $D_1R^{-/-}$ Mice

The effects of dopamine D_1/D_5R antagonists suggest that one or both of these receptors are essential for the induction of the L-LTP in the hippocampal CA1 area (Frey et al. 1991; Huang and Kandel 1995; Swanson-Park et al. 1999; O'Carroll and Morris 2004). To specifically establish the role of dopamine D_1 and D_5Rs in this process, we investigated whether L-LTP is impaired in $D_1R^{-/-}$ mice. We examined the magnitude of the enduring fEPSP potentiation (lasting at least 4 h) evoked by 3 trains of HFS at 10-min intervals and found that potentiation was significantly reduced in $D_1R^{-/-}$ mice compared with WT animals at various

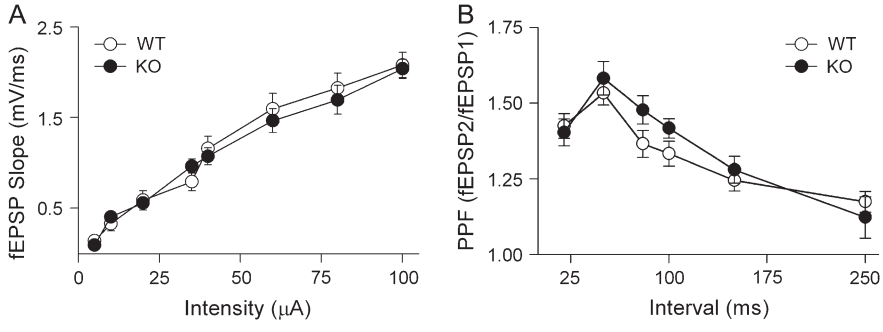

Figure 1. Baseline synaptic transmission is normal in $D_1R^{-/-}$ mice. (*A*) fEPSP slope values across stimulus intensities. Open circles indicate WT slices ($n = 14$), and filled circles indicate $D_1R^{-/-}$ slices ($n = 11$). (*B*) Paired-pulse facilitation ratio (second fEPSP slope/first fEPSP slope) evoked at different interstimulus intervals. WT (open circles, $n = 11$); $D_1R^{-/-}$ (filled circles, $n = 10$).

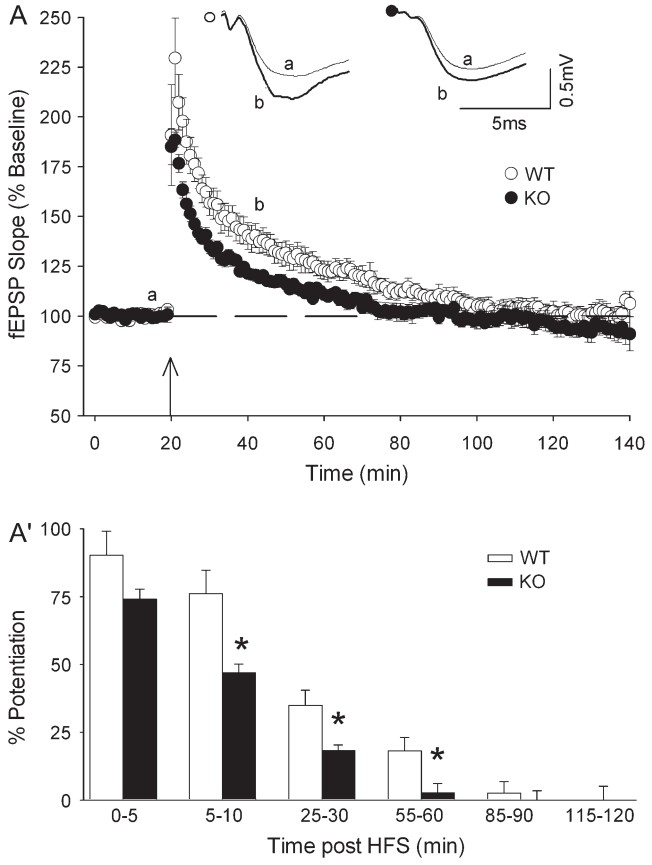

Figure 2. E-LTP magnitude is reduced in $D_1R^{-/-}$ mice. (*A*) Time course of fEPSP changes induced by a single HFS train (100 Hz, 1 s) applied (arrow) in slices from WT mice (open circles, $n = 6$) and $D_1R^{-/-}$ mice (filled circles, $n = 5$). The upper traces show representative averages of 8 consecutive fEPSPs recorded at the times indicated by the letters on the graph. (*A′*) Bars represent means ± standard error of mean of fEPSP potentiation recorded in 5-min periods after tetanus, taken from the data in (*A*) (* indicates $P < 0.05$, Student's *t*-test).

times after tetanus (Fig. 3*A*). Bonferroni post hoc analysis revealed significant differences in the magnitude of potentiation between $D_1R^{-/-}$ and WT animals beginning at 12 min after delivery of the third HFS train and persisting for at least 4 h after tetanus (Fig. 3*A′*). To determine whether D_5Rs also play a role in LTP, we analyzed the effects of a D_1/D_5 antagonist on LTP in WT and $D_1R^{-/-}$ mice. We did not find any significant effect of 0.1 μM SCH23390, a D_1/D_5 antagonist, on L-LTP in slices from $D_1R^{-/-}$ mice ($P > 0.05$, Fig. 3*B*). As expected, we did see an inhibitory effect of 0.1 μM SCH23390 on L-LTP in WT mice (Fig. 3*B′*). Higher concentrations of SCH23390 had no further effect on L-LTP in WT mice (at 1 h after tetanus, potentiation was 172 ± 11% in 0.1 μM SCH23390 and 175 ± 10% in 0.5–2 μM SCH23390; at 4 h after tetanus, potentiation was 129 ± 1% in 0.1 μM SCH23390 and 128 ± 12% in 0.5–2 μM SCH23390; $P > 0.05$). Thus, pharmacological blockade and genetic inactivation of D_1Rs have similar effects on L-LTP. Moreover, because SCH23390 does not further reduce the remaining L-LTP induced in $D_1R^{-/-}$ mice, we conclude that D_5Rs do not play a role in L-LTP at SC–CA1 synapses in the hippocampus.

D_1Rs Modulate NMDA-Mediated Postsynaptic Currents through a Protein Kinase A–Dependent Mechanism

Previous reports show that D_1R can interact with NR1 or NR2 subunits of NMDARs modulating its activity (Lee et al. 2002; Pei et al. 2004). Such interactions might explain the reduction of potentiation observed soon after the application of a train of HFS in $D_1R^{-/-}$ mice (see Fig. 2*A′*), which could affect the induction of LTP. We therefore investigated whether D_1Rs directly modulate NMDAR activity in hippocampal slices from $D_1R^{-/-}$ mice in pharmacologically isolated NMDAR-mediated EPSCs (see Materials and Methods). Under these conditions, superfusion with 50 μM SKF81297, a selective D_1/D_5 agonist, elicited an increase in EPSC amplitude (165 ± 18%; $n = 6$) (Fig. 4*A*, open circles) that was partially reversed during agonist washout (123 ± 17%; 50 min; $n = 6$) (Fig. 4*A*, open circles) in WT mice. This enhancement of the NMDA response in the presence of SKF81297 was different from the dopamine-induced decrease of NMDA-mediated fEPSP observed in hippocampus (Otmakhova and Lisman 1998b). The action of SKF81297 was specific for D_1/D_5R because 5 μM SCH23390, a selective antagonist of D_1/D_5R, blocked EPSC enhancement by SKF81297 (Fig. 4*A*, open squares; $n = 4$). Bath application of 50 μM AP5 completely suppressed this current (data not shown) indicating that these are NMDA-mediated EPSCs. The SKF81297-induced enhancement of NMDA-mediated EPSCs also occurred in $D_1R^{-/-}$ mice and reached a maximum value in approximately 18 min (129 ± 19%, $n = 6$) (Fig. 4*B*, filled circles). The potentiated EPSCs gradually decreased to control values after washout (107 ± 11%; 50 min; $n = 6$). The selective antagonist SCH23390 also blocked the induction of EPSC enhancement by SKF81297 in $D_1R^{-/-}$ mice (Fig. 4*B*, filled squares; $n = 4$). However, the mean amplitudes of EPSC enhancement in WT and $D_1R^{-/-}$ mice were significantly different during SKF81297 perfusion (149 ± 5% for WT vs. 125 ± 7% for $D_1R^{-/-}$ mice, $P < 0.01$, Fig. 4*C*) and after washout (127 ± 6% for WT vs. 108 ± 4% for $D_1R^{-/-}$ mice, $P < 0.05$, 30–40 min and 127 ± 7% for WT vs. 107 ± 3% for $D_1R^{-/-}$ mice, $P < 0.05$, 40–50 min, Fig. 4*C*). These data indicate that D_1Rs modulate NMDAR activity in the hippocampus.

D_1/D_5Rs are positively coupled to adenylyl cyclase and the protein kinase activated by cyclic adenosine 3′,5′-monophosphate (cAMP) (PKA) participates in both E-LTP and L-LTP (Frey et al. 1993; Blitzer et al. 1995; Abel et al. 1997; Otmakhova and Lisman 1998a). Therefore, we examined whether PKA is involved in D_1R regulation of NMDAR activity. Figure 4*D* shows the time course of SKF81297 (50 μM) effects in the presence of KT5720 (1 μM), a PKA inhibitor, perfused 20 min before and during SKF81297 application. KT5720 blocked SKF81297-induced enhancement of NMDA-mediated EPSCs in both WT and $D_1R^{-/-}$ mice (Fig. 4*D*), indicating that D_1Rs modulate NMDAR activity through a PKA-dependent mechanism.

$D_1R^{-/-}$ Mice Are Impaired in Spatial Learning and Memory in the Morris Water Maze

To investigate whether the decrease on hippocampal synaptic activity observed in $D_1R^{-/-}$ mice had any consequences in spatial learning, we tested $D_1R^{-/-}$ mice in the Morris water maze, a test known to require hippocampal function. Mice were trained to escape the water by swimming to a hidden platform guided by distal cues. Animals were first habituated to the water maze by introducing them into the pool. Mice were then given 4 training trials per day for 6 consecutive days. WT mice quickly learned to reach the platform as demonstrated by a progressive reduction in their escape latencies (Fig. 5), decreasing from an average of 40 s the first day to less than 8 s on day 6 (Fig. 5*A*, $P < 0.001$).

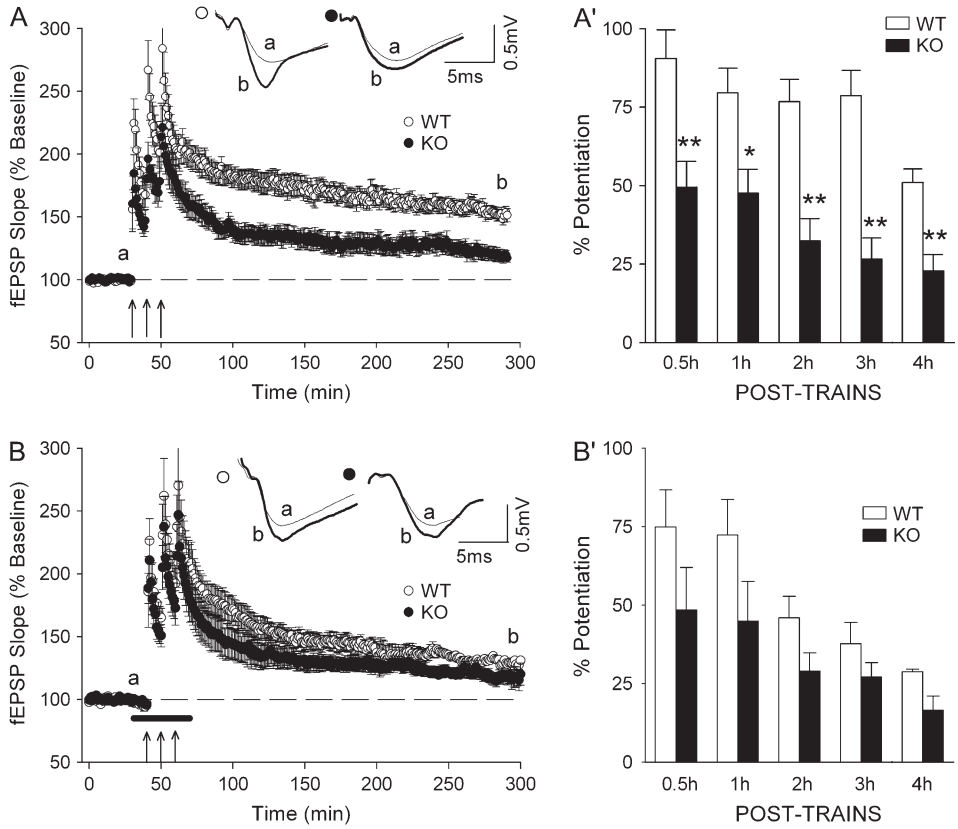

Figure 3. Genetic inactivation of D_1R has the same effect on L-LTP magnitude as pharmacological inhibition with a D_1/D_5R antagonist. (*A*) The plots summarize the time course of fEPSP changes induced by 3 HFS trains (arrows) in slices from WT (open circles, $n = 10$) and $D_1R^{-/-}$ (filled circles, $n = 6$) mice. (*A'*) Comparison of fEPSP potentiation level at different times after tetanus in the experiments shown in (*A*) (*$P < 0.05$, **$P < 0.01$; Bonferroni's test). (*B*, *B'*) show results of experiments similar to that depicted in (*A*, *A'*), respectively, but the tetanization protocol was delivered in the presence (horizontal filled bar) of 0.1 μM SCH23390, a D_1/D_5 antagonist. WT (open circles, $n = 5$) and $D_1R^{-/-}$ (filled circles, $n = 5$). The upper traces in (*A*, *B*) show representative averaged fEPSPs evoked at the indicated times during one representative experiment for each experimental condition.

Under the conditions used here, WT mice achieved the maximal decrease in escape latency by day 5. There were no differences in the escape latencies recorded on days 5 and 6. Extending the training period for a few more days did not cause any significant further reduction in the escape latency (data not shown). In sharp contrast, $D_1R^{-/-}$ mice showed an average escape latency of 40 s on the first day and 29 s on the sixth day. These mutant mice exhibited a significant decrease in escape time by the third day of training ($P < 0.05$) but were unable to further reduce the latency with additional training (Fig. 5*A*). These results indicate that WT mice progressively reduce their escape latencies, whereas $D_1R^{-/-}$ mice show no improvement after the third day, indicating a learning deficit in $D_1R^{-/-}$ mice ($P < 0.005$, Fig. 5*A*).

To evaluate long-term memory, we tested the mice in a retention probe trial, in which the submerged platform was removed. On the ninth day, 3 days after the end of the training period, we measured the time the mice spent in each quadrant of the pool ($n = 14$ per genotype). WT mice spent selectively more time in the target quadrant (53 ± 5%) compared with the first day of training (28 ± 4%) and to the other quadrants (Fig. 5*B*, $P < 0.001$). In contrast, $D_1R^{-/-}$ mice spent only 33.8 ± 2.3% of the time in the target quadrant on day 9 similar to the amount of time spent in this quadrant before training (27 ± 3%) and significantly less than WT animals on day 9 ($P < 0.01$). Thus, whereas WT mice increased the time spent in the target quadrant by 93%, $D_1R^{-/-}$ animals showed no significant increase, indicating impairment in learning and memory. We also analyzed the number of crosses through the platform location site in the probe trial (performed on day 9) for both genotypes and found that $D_1R^{-/-}$ mice performed significantly fewer crosses than WT mice (2.7 ± 0.6 for the $D_1R^{-/-}$ mice vs. 6.0 ± 0.9 for WT, $P < 0.01$; Fig. 5*C*). This suggests that $D_1R^{-/-}$ mice are unable to remember the precise location of the platform.

Next, we analyzed relearning using the reversal test. During the 3 days following the probe trial, animals were trained to locate the platform in a new location (diagonal to the previous position). WT animals quickly learned the new location of the platform as demonstrated by a progressive decrease in the latency time required to reach the platform over the 3 days of training. The initial average escape latency of 24.4 ± 3.0 s was reduced to an average of 9.5 ± 1.2 s on day 3 (Fig. 5*D*). In fact, WT animals only needed one training session to figure out the new location of the platform ($P < 0.01$, first vs. second and third day). By contrast, $D_1R^{-/-}$ mice were completely unable to learn the new location of the platform, and their escape latency did not vary much over the 3 days of retraining ($P < 0.25$, first vs. third day, Fig. 5*D*). However, in the cued test, (a hippocampus-independent task), both genotypes of mice were able to reach the platform with similar latency (Fig. 6*A*), and similar results were also found in the visual acuity test for the 2 type of mice, indicating that $D_1R^{-/-}$ mice have normal visual acuity and that both types of mice have similar motivation to find the platform.

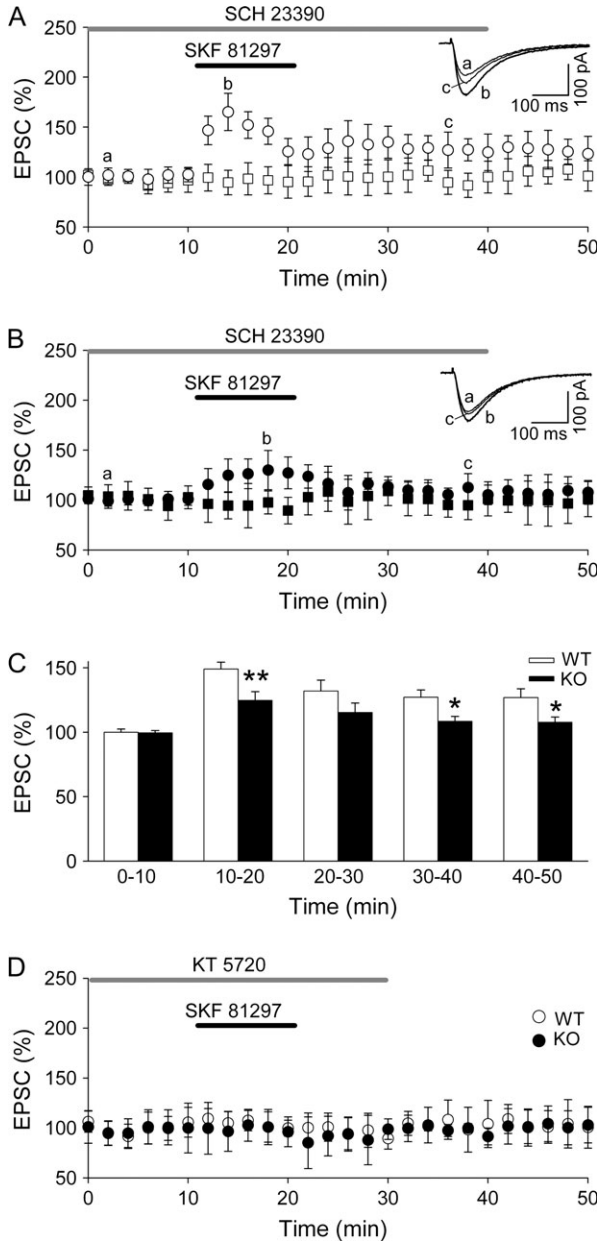

Figure 4. Inactivation of D_1R reduces the D_1/D_5R agonist–induced NMDA EPSC amplitude enhancement through a PKA-mediated mechanism. (*A*) Time course of 50 μM SKF81297 effects on normalized mean EPSC amplitudes evoked by SCC stimulation in control (open circles, $n = 6$) and in the presence of 5 μM SCH23390 (open squares, $n = 4$) in slices from WT mice. Inset shows averaged EPSCs ($n = 10$), recorded before (a), during (b), and after (c) SKF81297 perfusion in the absence of SCH23390. (*B*) Summary data and averaged EPSCs (inset) show the 50 μM SKF81297 effects in control (filled circles, $n = 6$) and in the presence of 5 μM SCH23390 (filled squares, $n = 4$) in slices from $D_1R^{-/-}$ mice. (*C*) Means of normalized EPSC amplitudes recorded in 10-min periods before and after SKF81297 perfusion in the absence of SCH23390 in WT and $D_1R^{-/-}$ mice, taken from the data in (*A*, *B*). Significant differences between WT and $D_1R^{-/-}$ mice were established at $*P < 0.05$ and $**P < 0.01$ (Student's *t*-test). (*D*) Summary data of 50 μM SKF81297 effects in the presence of 1 μM KT5720 in slices from WT (open circles, $n = 4$) and $D_1R^{-/-}$ mice (filled circle, $n = 4$). In all experiments, superfusion of drugs started 10 min before SKF81297 was applied, and values are given as the mean ± standard error of mean.

Locomotor Activity and Motor Coordination in $D_1R^{-/-}$ Mice

To test that the apparent learning deficit seen in $D_1R^{-/-}$ mice was not due to motor impairment, we measured basal locomotor activity and vertical movements. In agreement with previous results (Xu et al. 1994; Centonze et al. 2003; Rodrigues et al. 2007), we found that $D_1R^{-/-}$ mice were significantly more active than their WT littermates ($P < 0.001$, Fig. 6*B*), possibly due to the increase in glutamatergic activity found after D_1R inactivation (Rodrigues et al. 2007). Whereas WT mice scored an average of 4000 photocell beam crossings in a 60-min period, $D_1R^{-/-}$ mice had an average of 8000 crossings (Fig. 6*B*). However, vertical movements were similar in both genotypes (Fig. 6*C*). To test motor coordination, we used a rotarod test on 2 consecutive days and found no significant differences between WTs and $D_1R^{-/-}$ mice. These behavioral results show that inactivation of dopamine D_1Rs produces a specific impairment in spatial learning and memory processes, which cannot be attributed to aberrant motor behavior, abnormal visual acuity, or decreased motivation.

HFS-Induced Expression of Zif268 *and* arc *in the Hippocampus Is Blunted in Both $D_1R^{-/-}$ Mice and in WT Mice with Pharmacological Blockage of D_1Rs.*

We next examined the role of the D_1R in the induction of *zif268* and *Arc* elicited by high-frequency synaptic stimulation of the Schaffer collaterals in the hippocampus, the tetanization paradigm used to evoke L-LTP. The expression of these 2 genes is required for L-LTP for the consolidation of long-term memories (Guzowski et al. 2000; Jones et al. 2001; Kelley and Deadwyler, 2003) and for memory retrieval (Hall et al. 2001). In these experiments, fEPSPs were evoked and recorded every 15 s, and the tetanization protocol induced LTPs of similar magnitudes to those depicted in Figure 3. Basal expression of both Arc and Zif268 was obtained from hippocampal slices that were neither stimulated nor recorded (nonstimulated slices) but that were maintained in the recording chamber the same time than the slices undergoing tetanization. One hour after tetanic stimulation (3 trains of HFS at 10-min intervals) of Schaffer collaterals in hippocampal slices from WT mice, the expression of Zif268 and Arc in the pyramidal cells of the CA1 layer was significantly higher than in nonstimulated hippocampal sections (Fig. 7*C*,*G*). Although not all pyramidal cells respond to the tetanic stimulation with the same intensity, we found a large proportion of high-responding cells along the entire extension of the CA1 hippocampal area. Other neurons responded with lower levels of expression, and some show no increase in Zif268 or Arc expression. In sharp contrast, tetanic stimulation in hippocampal slices from the $D_1R^{-/-}$ mice does not induce Zif268 or Arc expression (Fig. 7, Table 1). Basal hippocampal expression of both proteins was similar in $D_1R^{-/-}$ and WT mice.

In order to further demonstrate that the effects we see in the $D_1R^{-/-}$ mice are exclusively due to the inactivation of D_1R rather than to any compensatory mechanisms secondary to D_1R deletion, we carry out similar experiments of gene expression after tetanic stimulation with pharmacological blockage of D_1R rather than genetic inactivation. We found that the presence of 0.5 μM SCH23390 in the bath solution (10 min before, during, and 10 min after HFS) not only inhibited the induction of LTP but also the Zif268 and Arc expression induced by tetanic stimulation in hippocampal sections from WT mice (Fig. 8, Table 1). These results were obtained in a series of 3 sets of experiments in which LTP and gene expression was measured in the same hippocampal slices. Indicating once more that D_1R activation is strictly necessary to produce the expression of some genes playing an essential role in L-LTP process.

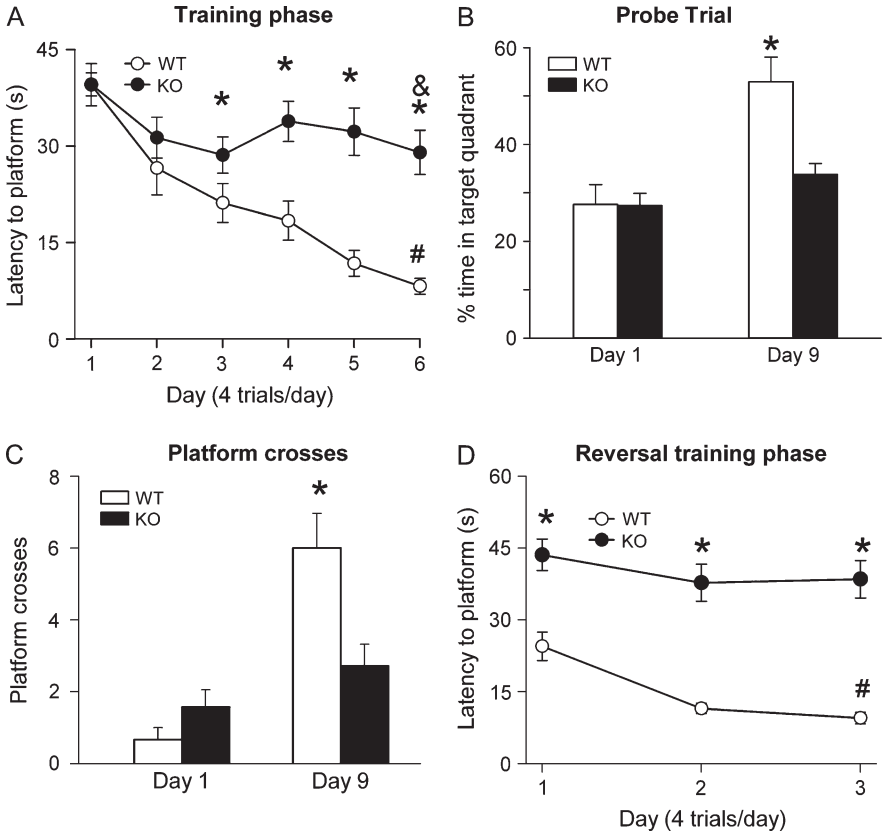

Figure 5. Hippocampus-dependent learning is impaired in dopamine $D_1R^{-/-}$ mice. (*A*) Escape latency during the training phase in the Morris water maze for WT and $D_1R^{-/-}$ mice. Data show the mean values ± standard error of mean, $*P < 0.005$, Tuckey's test. (*B*) Probe trial performed 3 days after the training phase to evaluate memory consolidation. Histograms represent the percentage of time spent in the target quadrants during the probe trial (60 s), $*P < 0.05$, Student's *t*-test. (*C*) Number of crosses over the former platform location during the probe trial in the beginning of the training phase (day 1) and in the probe trial (day 9), $*P < 0.01$, Student's *t*-test. (*D*) Escape latency during the relearning phase (60-s trials). For this test, the platform was located in the opposite quadrant to the training phase, $*P < 0.001$, $n = 15$, Tuckey's test.

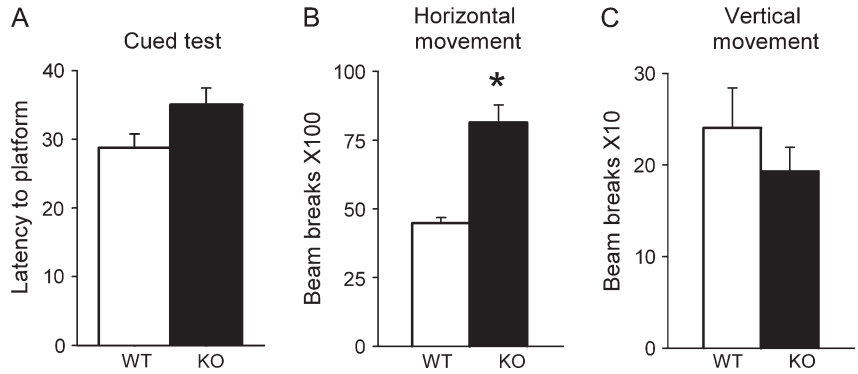

Figure 6. Locomotion and visual acuity are not impaired in $D_1R^{-/-}$ mice. Histograms illustrate (*A*) that $D_1R^{-/-}$ and WT mice have similar escape latencies with the visible platform in the Morris water maze, cued test. (*B*, *C*): horizontal (*B*) and vertical (*C*) locomotor activity during 60 min. ($*P < 0.001$, $n = 22$, Student's *t*-test).

Quantification of Zif268- and Arc-positive nuclei in hippocampal sections revealed that a moderate number of neurons express constitutive levels of both genes in the nonstimulated hippocampus of both genotypes (see Table 1). However, in WT mice, tetanic stimulation significantly increased positive nuclei by 20-fold for Zif268 and 6-fold for Arc. Tetanic stimulation did not increase the number of Zif268- or Arc-positive nuclei in $D_1R^{-/-}$ mice (an average of 179 ± 50 and 260 ± 89 positive nuclei per square millimeter for Zif268 and Arc, respectively) compared with nonstimulated slices (average of 128 ± 39 and 413 ± 28 for Zif268 and Arc, respectively). Pharmacological blockade of D_1R in stimulated sections from WT mice inhibited the increase in the number of Zif268- and Arc-positive nuclei induced after tetanus in a similar way that occurred in the $D_1R^{-/-}$ mice (Table 1). Altogether, these results indicate that the integrity of D_1Rs is critical for induction of these genes by tetanization in the rodent hippocampus.

Discussion

In this study, we show that $D_1R^{-/-}$ mice are significantly impaired in both E-LTP and L-LTP and showed a significant

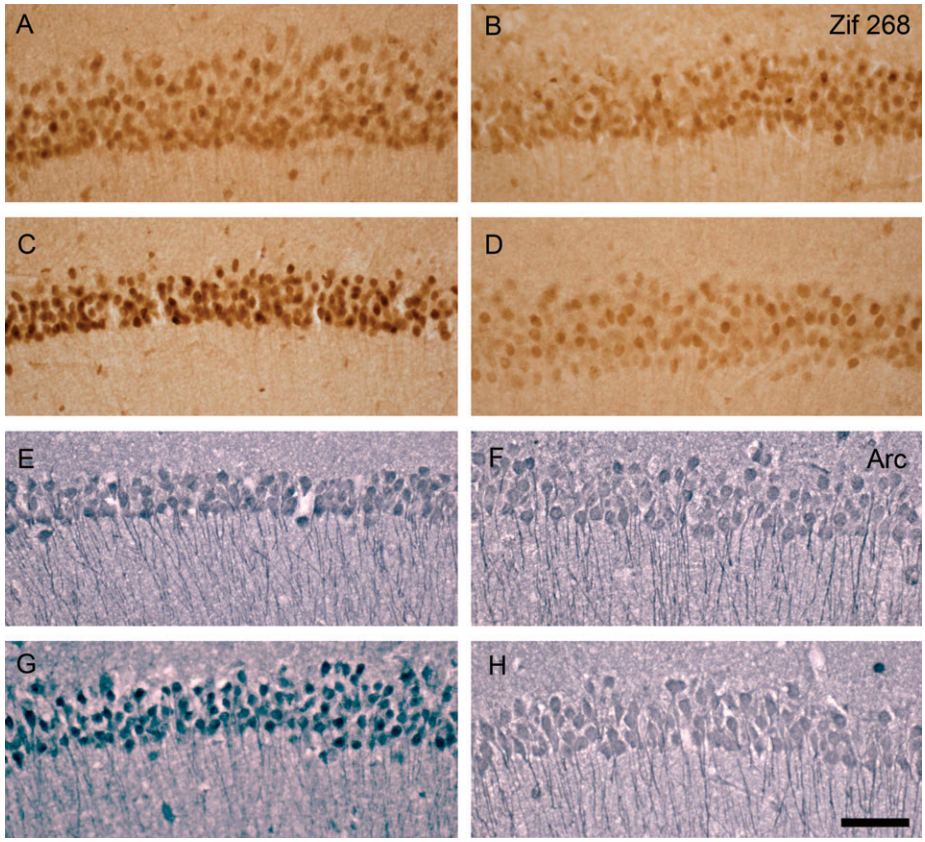

Figure 7. D_1R is required for activity-induced Zif268 and Arc expression in CA1 pyramidal cells after HFS of Schaffer collaterals. Photomicrographs of the CA1 pyramidal cell layer of the hippocampus from transverse brain slices of WT (*A*, *C*, *E*, and *G*) and $D_1R^{-/-}$ mice (*B*, *D*, *F*, and *H*) illustrating Zif268 (in brown) and Arc (in purple) expression in basal conditions (*A*, *B*, *E*, and *F*) and 1 h after HFS (*C*, *D*, *G*, and *H*). Bar indicates 50 μm.

reduction in the dopamine-induced potentiation of NMDA-mediated currents. We also show that the addition of SCH23390, a D_1/D_5 blocker, does not further reduced synaptic activity. Thus, we demonstrate that only the D_1Rs and not the D_5Rs are relevant for both forms of LTP. Moreover, there is no induction of *zif268* and *arc* following HFS in hippocampal slices from $D_1R^{-/-}$ mice and in those slices from WT mice treated with SCH23390. In addition, or perhaps as a direct consequence of reduced LTP, $D_1R^{-/-}$ mice exhibit impaired processing of spatial information in the Morris water maze confirming previous behavioral studies (Smith et al. 1998; El-Ghundi et al. 1999). Differences in genetic background do not account for this $D_1R^{-/-}$ phenotype because the WT and knockout mice used in this study are the littermate progeny of more than 10 heterozygous crossings. Although we cannot rule out the possibility of developmental compensation mechanisms, histochemical comparison of $D_1R^{-/-}$ and WT brain sections revealed no major differences (Xu et al. 1994; Moratalla et al. 1996).

Table 1
Quantification of HFS-induced Zif268 and Arc expression in hippocampal slices

	Zif268		Arc	
	WT	$D_1R^{-/-}$	WT	$D_1R^{-/-}$
Basal	163 ± 61	128 ± 39	372 ± 191	413 ± 28
HFS	3111 ± 250*	179 ± 50	2226 ± 432*	260 ± 89
	WT	SCH23390	WT	SCH23390
Basal	251 ± 94	337 ± 90	290 ± 92	160 ± 51
HFS	2000 ± 230*	311 ± 71	3100 ± 338*	250 ± 62

Note: Immunostained cells were counted in hippocampal sections (Figs 7 and 8) obtained from 3 (Arc) and 4 (Zif268) hippocampal slides, each from a different animal and with 4–7 sections each slice for $D_1R^{-/-}$ mice and its WT control mice, $n = 3$ (Arc) or $n = 4$ (Zif268). Counts for the D_1/D_5R blockage (SCH23390) experiment were obtained from 3 slices from 3 animals, 3 sections each, $n = 3$ (Arc and Zif268), for statistical purposes. Numbers indicate immunostained nuclei per square millimeter (mean ± standard error of mean).
*$P < 0.001$ compared with $D_1R^{-/-}$ or to SCH23390.

D_1Rs Facilitate E- and L-LTP in the Hippocampus

An important feature of our present work is the correlation of learning impairment with a severe reduction of hippocampal LTP and a blockage of LTP-induced gene expression in $D_1R^{-/-}$ mice. The ventral tegmental area (VTA) provides the dopaminergic innervation to the hippocampus, which in turn projects to VTA through a polysynaptic pathway. This functional loop has been proposed to participate in long-term memory processes (Lisman and Grace 2005). Thus, it is possible that the cognitive deficit found in $D_1R^{-/-}$ mice results from a deficit in dopaminergic neurotransmission in the hippocampal–VTA loop. In fact, we found several alterations in hippocampal synaptic plasticity in $D_1R^{-/-}$ mice that might explain such a deficit. $D_1R^{-/-}$ mice display a reduced level of potentiation in both E- and L-LTP and in the positive modulation of NMDAR-mediated current by D_1R activation. Our results are in agreement with previous experiments carried out in hippocampal slices from another line of $D_1R^{-/-}$ mice, which showed that D_1Rs are involved in L-LTP maintenance (Matthies et al. 1997). Four hours after the tetanization protocol in $D_1R^{-/-}$ slices, these authors observed a remnant

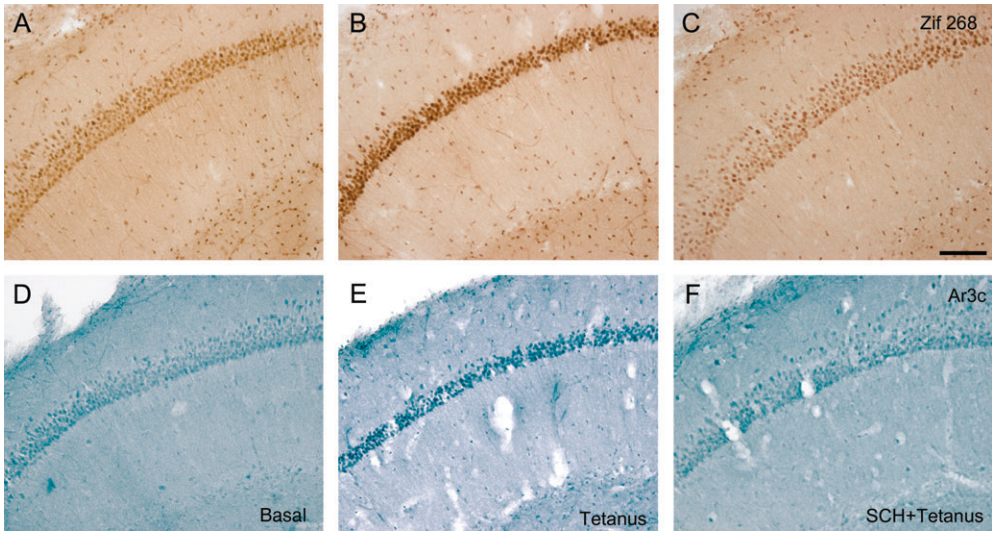

Figure 8. D_1R antagonist SCH23390 blocked LTP-induced Zif268 and Arc expression in CA1 pyramidal cells. Photomicrographs of the CA1 pyramidal cell layer of the hippocampus from transverse brain slices of WT animals illustrating Zif268 (in brown) and Arc (in purple) expression in basal conditions (*A*, *D*), 1 h after HFS (*B*, *E*), and 1 h after HFS in the presence of 0.5 μM SCH23390, a D_1/D_5R antagonist (*C*, *F*). Note the inhibition of Zif268- and Arc-induced expression by LTP in the presence of SCH23390. Bar indicates 100 μm.

potentiation of similar magnitude to that found in our experiments with mutant mice or SCH23390-treated WT mice. This result contrasts with the faster decay of hippocampal L-LTP toward baseline described by other groups when using the D_1/D_5 antagonist, SCH23390 (Frey et al. 1991; Huang and Kandel 1995; Swanson-Park et al. 1999). This discrepancy might be explained in base of species differences because these previous works were conducted in rat hippocampal slices, whereas our results have been obtained from mouse hippocampal slices. In fact, we have also found in rat hippocampal slices that L-LTP maintenance was totally inhibited when 3 trains of HFS were applied in the presence of SCH23390 (Suárez LM, Solís JM, unpublished data).

Our work not only confirms the previous work of Matthies et al. (1997) but also extends it in very significant ways. 1) We found that SCH23390 does not further reduce L-LTP in $D_1R^{-/-}$ mice, demonstrating that D_5Rs do not participate in this form of synaptic plasticity. This result is surprising considering that, although rat hippocampal pyramidal neurons express both receptor subtypes, D_5R is the predominant one (Bergson et al. 1995; Smith et al. 2005). The distinct subcellular distribution of these 2 receptors in hippocampal neurons supports our findings. D_5Rs are mainly localized in the cell soma (Liu et al. 2000; Rivera et al. 2002; Smith et al. 2005) where they can interact with $GABA_A$ receptors (Liu et al. 2000). By contrast, D_1Rs are predominantly localized in dendritic spines (Huang et al. 1992; Bergson et al. 1995; Smith et al. 2005). NMDARs are also localized in dendrite spines of hippocampal neurons, as are the molecules for signal transduction and local protein synthesis that are crucial for induction of L-LTP. 2) More importantly, we show that absence of D_1Rs also reduces the magnitude of E-LTP and its duration. Not much attention has been paid to the role of dopamine in hippocampal E-LTP (Huang and Kandel 1995), although some authors (Otmakhova and Lisman 1996), using a D_1/D_5R antagonist, have presented evidence indicating that these receptors positively modulate E-LTP induction. Our results are consistent with this view, demonstrating for the first time that D_1R activation is also required for the full expression of E-LTP. Thus, we propose that D_1R, but not D_5R, are relevant for both forms of LTP. 3) In addition, we found that D_1R activation potentiates NMDAR-mediated synaptic currents by a mechanism requiring PKA activation. This result is similar to that reported by others in striatal neurons (Flores-Hernandez et al. 2002) but different from the D_1/D_5R-mediated potentiation of NMDA currents observed in prefrontal neurons, which is independent of the classical PKA pathway (Chen et al. 2004). We also found that in $D_1R^{-/-}$ mice, a D_1/D_5R agonist is still able to moderately enhance NMDA currents by a mechanism blocked by a D_1/D_5R antagonist, indicating that at least the massive activation of D_5Rs can also modulate NMDAR via the PKA signaling cascade. Interestingly, in the presence of D_1/D_5R agonist, there is a gradual reduction in NMDA currents after washout that might indicate a mechanism for partial turnoff, such as desensitization. This mechanism could have interesting functional consequences, and further studies are required to determine the significance of this finding.

Possible Mechanisms of D_1R-Induced Synaptic Facilitation

The mechanism by which D_1R modulates different phases of LTP is not well understood. We suspect that D_1R could augment E- and L-LTP by different mechanisms because E-LTP is rapidly developed and does not require protein synthesis, whereas L-LTP does. Nevertheless, cAMP synthesis promoted by D_1R activation could underlie both of them: whereas D_1R-induced potentiation of NMDA currents might well facilitate the primary steps involved in the induction mechanisms of E-LTP, a stronger activation of D_1R in L-LTP could allow a cross talk between different kinases converging in the mitogen activated protein kinase/extracellular signal-regulated kinase signaling pathway to trigger the required macromolecular synthesis at tagged synapses (Kelleher et al. 2004).

It is also possible that the D_1R participates in LTP via functional protein–protein interactions with glutamate receptors. D_1R can physically interact with NR1 or NR2A subunits of NMDARs and modulate NMDAR activity (Lee et al. 2002; Pei et al. 2004). The coactivation of these 2 receptors stimulates protein synthesis, upregulates GluR1 receptor subunit, and

increases surface expression of GluR1 subunit of AMPA receptors at synaptic sites (Smith et al. 2005). The trafficking of GluR1 subunits to the appropriate synapses has been implicated in associative learning and L-LTP induction (Passafaro et al. 2001; Rumpel et al. 2005). Thus, increased expression and specific trafficking of GluR1 could very well be the mechanism by which D_1R activation augments L-LTP.

Hippocampal-Dependent Learning Is Impaired in $D_1R^{-/-}$ Mice

Because spatial learning and memory storage induce hippocampal LTP (Pastalkova et al. 2006; Whitlock et al. 2006) and due to the drastic reduction of LTP in our $D_1R^{-/-}$ mice, we expected to find an impairment in spatial learning. Indeed, we found that $D_1R^{-/-}$ mice do reduce escape latency in the water maze between the 1st and the 3rd day but are unable to further reduce it over 3 additional days of training, as have been shown previously (Smith et al. 1998; El-Ghundi et al. 1999). This suggests that the knockout mice understand the task but are unable to acquire a navigation strategy to further reduce escape latency. This inability could not be attributed to poor swimming skill because swimming speed was similar in WT and KO mice, and KO mice are more active than WT. Impairment could also be due to lack of motivation to escape the water because the dopamine system is very important for motivated behavior. However, $D_1R^{-/-}$ and WT mice have similar escape latencies in the cued trial, demonstrating that $D_1R^{-/-}$ mice have no deficit in visual acuity, locomotion, or motivation to escape the water. These results strongly suggest that D_1R inactivation produces a specific impairment in spatial learning and memory.

D_1Rs Are Required for HFS-Induced Expression of Zif268 and Arc

The striking induction of Zif268 and Arc that occurs in CA1 pyramidal cells in the hippocampus after HFS trains is completely absent in $D_1R^{-/-}$ animals. This inhibition correlates with the deficit in LTP and the loss of spatial learning and memory consolidation in these mutant mice, strongly suggesting that they are all caused by the lack of D_1Rs. Our results are consistent with previous data showing that disruption of *zif268* or *arc* expression blocks long-term memory and L-LTP (Davis et al. 2000; Guzowski et al. 2000; Jones et al. 2001). In addition, the lack of Zif268 and Arc expression after HFS in $D_1R^{-/-}$ indicates that the signaling mechanisms linking synaptic activation in the dendrites with nuclear gene expression are recruited upon D_1R activation. The fact that pharmacological blockade of D_1R inhibits the LTP-induced gene expression as happens with the genetic inactivation of D_1R in the knockout mice strongly indicates that D_1Rs are critical for the proteins synthesis required for the transition from E-LTP to L-LTP and that this effect is not due to any compensatory mechanisms during $D_1R^{-/-}$ mice development. The expression of Arc after HFS in WT is particularly notable because newly synthesized *arc* mRNA is selectively targeted to activated synapses by an NMDAR-dependent process (Steward et al. 1998; Rodriguez et al. 2005). Thus, both NMDAR and D_1R are required for the activity-dependent induction and synaptic targeting of *arc*, suggesting that *arc* is part of the mechanism that integrates signals from these 2 receptors to produce changes in synaptic efficacy. Finally, although genetic inactivation of D_1Rs markedly reduces E- and L-LTP, both phases of LTP are still present to some degree in $D_1R^{-/-}$ animals. Our studies suggest that this residual LTP is not sufficient to induce Zif268 or Arc expression or to support spatial learning in the Morris water maze, suggesting that the modulatory action of D_1R is critical for the presumed behavioral consequences of LTP.

The data presented here provide strong evidence that D_1Rs are critical for the induction of translational events at selected synapses underlying L-LTP and memory consolidation. In the ongoing debate about how LTP mechanisms are involved in learning and memory formation, our findings provide important evidence suggesting that L-LTP, spatial memory formation, and activity-dependent gene expression share molecular mechanisms triggered by D_1R activation.

Notes

Funded by the Spanish Ministerio de Ciencia y Tecnología, SAF2003-4864, GEN2003-C06-02/NAC, Fondo de Investigación Sanitaria FIS 03/1004, RTA G03/05, and PNSD (RM); Ministerio de Sanidad y Consumo, PI05/1194 (JMS); and PI041226 and Fundación "La Caixa" (VC); Fibio-HRC, B-23/2005 (LMS); Gobierno Vasco (OO); and FPI (NG) and Programa Ramón y Cajal del Ministerio de Educación y Ciencia (EDM). Centro de Investigation Biomédica en Red de enfermedades Neurodegenerativas, Instituto de Salud Carlos III, Madrid, Spain (RM, VC, EDM). *Conflict of Interest*: None declared.

Funding to pay the Open Access publication charges for this article was provided by Ministerio de Ciencia y Tecnología, SAF2003-4864, GEN2003-C06-02/NAC.

Address correspondence to Rosario Moratalla, Instituto Cajal, Consejo Superior de Investigaciones Científicas, Avda Dr Arce 37, 28002 Madrid, Spain. Email: moratalla@cajal.csic.es.

References

Abel T, Nguyen PV, Barad M, Deuel TA, Kandel ER, Bourtchouladze R. 1997. Genetic demonstration of a role for PKA in the late phase of LTP and in hippocampus-based long-term memory. Cell. 88:615–626.

Bergson C, Mrzljak L, Smiley JF, Pappy M, Levenson R, Goldman-Rakic PS. 1995. Regional, cellular, and subcellular variations in the distribution of D1 and D5 dopamine receptors in primate brain. J Neurosci. 15:7821–7836.

Blitzer RD, Wong T, Nouranifar R, Iyengar R, Landau EM. 1995. Postsynaptic cAMP pathway gates early LTP in hippocampal CA1 region. Neuron. 15:1403–1414.

Calabresi P, Maj R, Pisani A, Mercuri NB, Bernardi G. 1992. Long-term synaptic depression in the striatum: physiological and pharmacological characterization. J Neurosci. 12:4224–4233.

Centonze D, Grande C, Saulle E, Martin AB, Gubellini P, Pavon N, Pisani A, Bernardi G, Moratalla R, Calabresi P. 2003. Distinct roles of D1 and D5 dopamine receptors in motor activity and striatal synaptic plasticity. J Neurosci. 23:8506–8512.

Chen G, Greengard P, Yan Z. 2004. Potentiation of NMDA receptor currents by dopamine D1 receptors in prefrontal cortex. Proc Natl Acad Sci USA. 101:2596–2600.

Davis S, Vanhoutte P, Pages C, Caboche J, Laroche S. 2000. The MAPK/ERK cascade targets both Elk-1 and cAMP response element-binding protein to control long-term potentiation-dependent gene expression in the dentate gyrus in vivo. J Neurosci. 20:4563–4572.

El-Ghundi M, Fletcher PJ, Drago J, Sibley DR, O'Down BF, George SR. 1999. Spatial learning deficit in dopamine D1 receptor knockout mice. Eur J Pharmacol. 383:95–106.

Flores-Hernandez J, Cepeda C, Hernandez-Echeagaray E, Calvert CR, Jokel ES, Fienberg AA, Greengard P, Levine MS. 2002. Dopamine enhancement of NMDA currents in dissociated medium-sized striatal neurons: role of D1 receptors and DARPP-32. J Neurophysiol. 88:3010–3020.

Frey U, Huang YY, Kandel ER. 1993. Effects of cAMP simulate a late stage of LTP in hippocampal CA1 neurons. Science. 260:1661–1664.

Frey U, Matthies H, Reymann KG, Matthies H. 1991. The effect of dopaminergic D1 receptor blockade during tetanization on the expression of long-term potentiation in the rat CA1 region in vitro. Neurosci Lett. 129:111–114.

Grande C, Zhu H, Martín AB, Lee M, Ortíz O, Hiroi N, Moratalla R. 2004. Chronic treatment with atypical neuroleptics induces striosomal FosB/DeltaFosB expression in rats. Biol Psychiatry. 55:457–463.
Gurden H, Tassin JP, Jay TM. 1999. Integrity of the mesocortical dopaminergic system is necessary for complete expression of in vivo hippocampal-prefrontal cortex long-term potentiation. Neuroscience. 94:1019–1027.
Guzowski JF, Lyford GL, Stevenson GD, Houston FP, McGaugh JL, Worley PF, Barnes CA. 2000. Inhibition of activity-dependent arc protein expression in the rat hippocampus impairs the maintenance of long-term potentiation and the consolidation of long-term memory. J Neurosci. 20:3993–4001.
Hall J, Thomas KL, Everitt BJ. 2001. Cellular imaging of zif268 expression in the hippocampus and amygdala during contextual and cued fear memory retrieval: selective activation of hippocampal CA1 neurons during the recall of contextual memories. J Neurosci. 21:2186–2193.
Huang Q, Zhou D, Chase K, Gusella JF, Aronin N, DiFiglia M. 1992. Immunohistochemical localization of the D1 dopamine receptor in rat brain reveals its axonal transport, pre- and postsynaptic localization, and prevalence in the basal ganglia, limbic system, and thalamic reticular nucleus. Proc Natl Acad Sci USA. 89:11988–11992.
Huang YY, Kandel ER. 1995. D1/D5 receptor agonists induce a protein synthesis-dependent late potentiation in the CA1 region of the hippocampus. Proc Natl Acad Sci USA. 92:2446–2450.
Huang YY, Simpson E, Kellendonk C, Kandel ER. 2004. Genetic evidence for the bidirectional modulation of synaptic plasticity in the prefrontal cortex by D1 receptors. Proc Natl Acad Sci USA. 101:3236–3241
Isaacson JS, Solis JM, Nicoll RA. 1993. Local and diffuse synaptic actions of GABA in the hippocampus. Neuron. 10:165–175.
Jones MW, Errington ML, French PJ, Fine A, Bliss TV, Garel S, Charnay P, Bozon B, Laroche S, Davis S. 2001. A requirement for the immediate early gene Zif268 in the expression of late LTP and long-term memories. Nat Neurosci. 4:289–296.
Kelleher RJ 3rd, Govindarajan A, Jung HY, Kang H, Tonegawa S. 2004. Translational control by MAPK signaling in long-term synaptic plasticity and memory. Cell. 116:467–479.
Kelly MP, Deadwyler SA. 2003. Experience-dependent regulation of the immediate-early gene arc differs across brain regions. J Neurosci. 23:6443–6451.
Konradi C, Leveque JC, Hyman SE. 1996. Amphetamine and dopamine-induced immediate early gene expression in striatal neurons depends on postsynaptic NMDA receptors and calcium. J Neurosci. 16:4231–4239.
Lamberty Y, Gower AJ. 1990. Age-related changes in spontaneous behavior and learning in NMRI mice from maturity to middle age. Physiol Behav. 47:1137–1144.
Lee FJ, Xue S, Pei L, Vukusic B, Chery N, Wang Y, Wang YT, Niznik HB, Yu XM, Liu F. 2002. Dual regulation of NMDA receptor functions by direct protein-protein interactions with the dopamine D1 receptor. Cell. 18:219–230.
Lemon N, Manahan-Vaughan D. 2006. Dopamine D1/D5 receptors gate the acquisition of novel information through hippocampal long-term potentiation and long-term depression. J Neurosci. 26:7723–7729.
Li S, Cullen WK, Anwyl R, Rowan MJ. 2003. Dopamine-dependent facilitation of LTP induction in hippocampal CA1 by exposure to spatial novelty. Nat Neurosci. 6:526–531.
Lisman JE, Grace AA. 2005. The hippocampal-VTA loop: controlling the entry of information into long-term memory. Neuron. 46:703–713.
Liu F, Wan Q, Pristupa ZB, Yu XM, Wang YT, Niznik HB. 2000. Direct protein-protein coupling enables cross-talk between dopamine D5 and gamma-aminobutyric acid A receptors. Nature. 20:274–280.
Ljungberg T, Apicella P, Schultz W. 1992. Responses of monkey dopamine neurons during learning of behavioral reactions. J Neurophysiol. 67:145–163.
Malenka RC, Bear MF. 2004. LTP and LTD: an embarrassment of riches. Neuron. 44:5–21.
Martin ED, Buño W. 2003. Caffeine-mediated presynaptic long-term potentiation in hippocampal CA1 pyramidal neurons. J Neurophysiol. 89:3029–3038.
Matthies H, Becker A, Schroeder H, Kraus J, Hollt V, Krug M. 1997. Dopamine D1-deficient mutant mice do not express the late phase of hippocampal long-term potentiation. Neuroreport. 8: 3533–3535.
Moratalla R, Robertson HA, Graybiel AM. 1992. Dynamic regulation of NGFI-A (zif268, egr1) gene expression in the striatum. J Neurosci. 12:2609–2622.
Moratalla R, Xu M, Tonegawa S, Graybiel AM. 1996. Cellular responses to psychomotor stimulant and neuroleptic drugs are abnormal in mice lacking the D1 dopamine receptor. Proc Natl Acad Sci USA. 93:14928–14933.
O'Carroll CM, Morris RG. 2004. Heterosynaptic co-activation of glutamatergic and dopaminergic afferents is required to induce persistent long-term potentiation. Neuropharmacology. 47:324–332.
Otmakhova NA, Lisman JE. 1996. D1/D5 dopamine receptor activation increases the magnitude of early long-term potentiation at CA1 hippocampal synapses. J Neurosci. 16:7478–7486.
Otmakhova NA, Lisman JE. 1998a. D1/D5 dopamine receptors inhibit depotentiation at CA1 synapses via cAMP-dependent mechanism. J Neurosci. 18:1270–1279.
Otmakhova NA, Lisman JE. 1998b. Dopamine selectively inhibits the direct cortical pathway to the CA1 hippocampal region. J Neurosci. 19:1437–1445.
Passafaro M, Piech V, Sheng M. 2001. Subunit-specific temporal and spatial patterns of AMPA receptor exocytosis in hippocampal neurons. Nat Neurosci. 9:917–926.
Pastalkova E, Serrano P, Pinkhasova D, Wallace E, Fenton AA, Sacktor TC. 2006. Storage of spatial information by the maintenance mechanism of LTP. Science. 313:1141–1144.
Pavón N, Martín AB, Mendialdua A, Moratalla R. 2006. ERK phosphorylation and FosB expression are associated with L-DOPA-induced dyskinesia in hemiparkinsonian mice. Biol Psychiatry. 59:64–74.
Pei L, Lee FJ, Moszczynska A, Vukusic B, Liu F. 2004. Regulation of dopamine D1 receptor function by physical interaction with the NMDA receptors. J Neurosci. 4:1149–1158.
Picconi B, Centonze D, Hakansson K, Bernardi G, Greengard P, Fisone G, Cenci MA, Calabresi P. 2003. Loss of bidirectional striatal synaptic plasticity in L-DOPA-induced dyskinesia. Nat Neurosci. 6: 501–506.
Rivera A, Alberti I, Martin AB, Narvaez JA, de la Calle A, Moratalla R. 2002. Molecular phenotype of rat striatal neurons expressing the dopamine D5 receptor subtype. Eur J Neurosci. 16:2049–2058.
Rodrigues TB, Granado N, Ortiz O, Cerdán S, Moratalla R. Forthcoming. The metabolic interactions between glutamatergic and dopaminergic neurotransmitter systems are mediated through D_1 dopamine receptors. J Neurosci Res.
Rodriguez JJ, Davies HA, Silva AT, De Souza IE, Peddie CJ, Colyer FM, Lancashire CL, Fine A, Errington ML, Bliss TV, et al. 2005. Long-term potentiation in the rat dentate gyrus is associated with enhanced Arc/Arg3.1 protein expression in spines, dendrites and glia. Eur J Neurosci. 21:2384–2396.
Rumpel S, LeDoux J, Zador A, Malinow R. 2005. Postsynaptic receptor trafficking underlying a form of associative learning. Science. 308:83–88.
Sajikumar S, Navakkode S, Frey JU. 2005. Protein synthesis-dependent long-term functional plasticity: methods and techniques. Curr Opin Neurobiol. 15:607–613.
Smith DR, Striplin CD, Geller AM, Mailman RB, Drago J, Lawler CP, Gallagher M. 1998. Behavioural assessment of mice lacking D1A dopamine receptors. Neuroscience. 86:135–146.
Smith WB, Starck SR, Roberts RW, Schuman EM. 2005. Dopaminergic stimulation of local protein synthesis enhances surface expression of GluR1 and synaptic transmission in hippocampal neurons. Neuron. 3:765–779.
Steward O, Wallace CS, Lyford GL, Worley PF. 1998. Synaptic activation causes the mRNA for the IEG arc to localize selectively near activated postsynaptic sites on dendrites. Neuron. 21: 741–751.
Swanson-Park JL, Coussens CM, Mason-Parker SE, Raymond CR, Hargreaves EL, Dragunow M, Cohen AS, Abraham WC. 1999. A double dissociation within the hippocampus of dopamine D1/D5

receptor and beta-adrenergic receptor contributions to the persistence of long-term potentiation. Neuroscience. 92:485–497.
Tan A, Moratalla R, Lyford GL, Worley P, Graybiel AM. 2000. The activity-regulated cytoskeletal-associated protein arc is expressed in different striosome-matrix patterns following exposure to amphetamine and cocaine. J Neurochem. 74:2074–2078.
Whishaw IQ, Dunnett SB. 1985. Dopamine depletion, stimulation or blockade in the rat disrupts spatial navigation and locomotion dependent upon beacon or distal cues. Behav Brain Res. 18:11–29.
Whitlock JR, Heynen AJ, Shuler MG, Bear MF. 2006. Learning induces long-term potentiation in the hippocampus. Science. 313:1093–1097
Williams GV, Goldman-Rakic PS. 1995. Modulation of memory fields by dopamine D1 receptors in prefrontal cortex. Nature. 376:572–575.
Xu M, Moratalla R, Gold LH, Hiroi N, Koob GF, Graybiel AM, Tonegawa S. 1994. Dopamine D1 receptor mutant mice are deficient in striatal expression of dynorphin and in dopamine-mediated behavioral responses. Cell. 79:729–742.